



Pergamon

Crystal Engineering 5 (2002) 265–272

**Crystal
Engineering**

www.elsevier.com/locate/cryseng

Orientation imaging microscopy analysis of bulk, melt-textured YBCO superconductors

A. Koblischka-Veneva^{a,*}, M.R. Koblischka^b, K. Ogasawara^c,
M. Murakami^c

^a *Institute of Functional Materials, University of the Saarland, P.O. Box 151150, D-66041 Saarbrücken, Germany*

^b *Institute of Experimental Physics, University of the Saarland, P.O. Box 151150, D-66041 Saarbrücken, Germany*

^c *SRL/ISTEC, Div. III, 1-16-25 Shibaura, Minato-ku, Tokyo 105-0023, Japan*

Abstract

In this contribution, we apply orientation imaging microscopy (OIM) to melt-textured, bulk $\text{YBa}_2\text{Cu}_3\text{O}_y$ (YBCO) samples, which require to perform an automated two-phase analysis. Both YBCO and the green phase Y_2BaCuO_5 (Y-211) are of orthorhombic crystal structures, but with clearly distinct unit cell parameters. We obtain the orientations of the individual crystallites and the misorientation distributions for both YBCO and Y-211. From the obtained data, we calculate the orientation distribution functions.

© 2003 Elsevier Science Ltd. All rights reserved.

Keywords: Melt-texturing; YBCO; OIM analysis; Grain orientation

1. Introduction

Melt-texturing of $\text{YBa}_2\text{Cu}_3\text{O}_y$ (YBCO) is a very important means to produce large bulk disk-shaped samples, which are used in a variety of applications unique to high- T_c superconductors, like e.g. flywheels, rotors of electromotors, etc. [1]. However, the control of the growth process conditions is essential in order to create homogeneous, monolithic samples with a large number of intrinsic flux pinning centres. Especially the presence of grain and subgrain boundaries poses a large problem in high magnetic

* Corresponding author. Tel.: +49-681-3023408; fax: +49-681-3024876.

E-mail address: a.koblischka-veneava@mx.uni-saarland.d (A. Koblischka-Veneva).

field applications [2,3]. This type of sample can be very well analysed by means of orientation imaging (OIM or sometimes called electron-backscatter diffraction, EBSD), but it is essential that a two-phase analysis is performed as the melt-textured YBCO samples contain a certain amount of green phase particles (Y_2BaCuO_5 , Y-211), which play a major role as flux pinning centres. Both YBCO and Y-211 have orthorhombic unit cells, but with clearly distinct crystal parameters. The OIM analysis is a powerful tool to obtain the local crystallographic orientations, thus enabling a visualisation and determination of the microstructural properties [4,5]. Up to now, only one single experiment on melt-textured samples was published in the literature [6], which, however, showed serious difficulties concerning the Kikuchi pattern quality, thus not allowing mapping to be performed. In this contribution, we present the results of such a two-phase analysis on a typical melt-textured YBCO sample.

2. Experimental

Melt-textured YBCO samples were produced using the standard procedure [7]. To the YBCO starting powder, an additional amount of 20 vol.-% Y-211 powder is added prior to the melt-texturing. An additional oxygen treatment is required to obtain superconducting YBCO. For the OIM analysis, small pieces were cut from the bulk pellets to a nearly cubic shape with 1.5 mm edge length. The samples were subsequently dry polished using 3M polishing papers as described in Ref. [8], using ethanol for cleaning purposes. This procedure was demonstrated to work well on various polycrystalline YBCO samples [8].

As EBSD system, we employ a CamScan series 4 microscope equipped with a TSL OIM analysis unit [9]. The Kikuchi patterns are generated at an acceleration voltage of 25 KV, recorded by means of a low-light CCD camera. The typical recording speed of our EBSD system is of the order of 1–2 s/pattern; in the case of a two-phase scan the time may be slightly longer. To produce a crystallographic orientation map, the electron beam is scanned over a selected surface area and the resulting Kikuchi patterns are automatically indexed and analyzed (i.e. the Kikuchi bands are detected by means of the software). These data are then further analyzed using the analysis software package. For a proper OIM scan of such a melt-textured sample, a two-phase scan must be performed, where the major phase is YBCO and the secondary phase Y-211. The OIM software enables such a scan with different phases; the measure for the controlling computer to check for the secondary phase is the confidence index (CI), which is determined to each indexation of a Kikuchi pattern. If a user-specified value for the minimum CI is underrun, the computer will attempt an indexation of the pattern with the secondary phase. In this way, a two-phase map can be produced, yielding e.g. information about the phase boundaries and the phase distribution.

3. Results and discussion

Fig. 1 presents the Kikuchi patterns and indexing of YBCO (a) and the Y-211 phase (b). In the case of the YBCO pattern indexed with the maximum confidence index $CI = 1$, we obtain the Euler angles $\phi_1 = 22.92^\circ$, $\Phi = 9.78^\circ$ and $\phi_2 = 96.06^\circ$ corresponding to a (0 0 1) orientation showing the (0 0 1) star in the upper part of the pattern. For Y-211 we find (also with $CI = 1$) $\phi_1 = 88.62^\circ$, $\Phi = 90^\circ$ and $\phi_2 = 286.72^\circ$, with the (-1 0 1) pole on the lower left side of the pattern.

The OIM results can be presented in maps (Fig. 2), separately for the two phases. The first map (a) is a phase map, where the YBCO is represented in dark grey, and the green phase in light grey. Only a minor fraction (YBCO—98.6%, Y-211—1.4%) of green phase was detected here. Maps (b), (c) and (d) present inverse pole figure maps in all three crystallographic directions [0 0 1], [1 0 0] and [1 1 0] of this sample for both YBCO and the Y-211 phase together. The orientations are given in

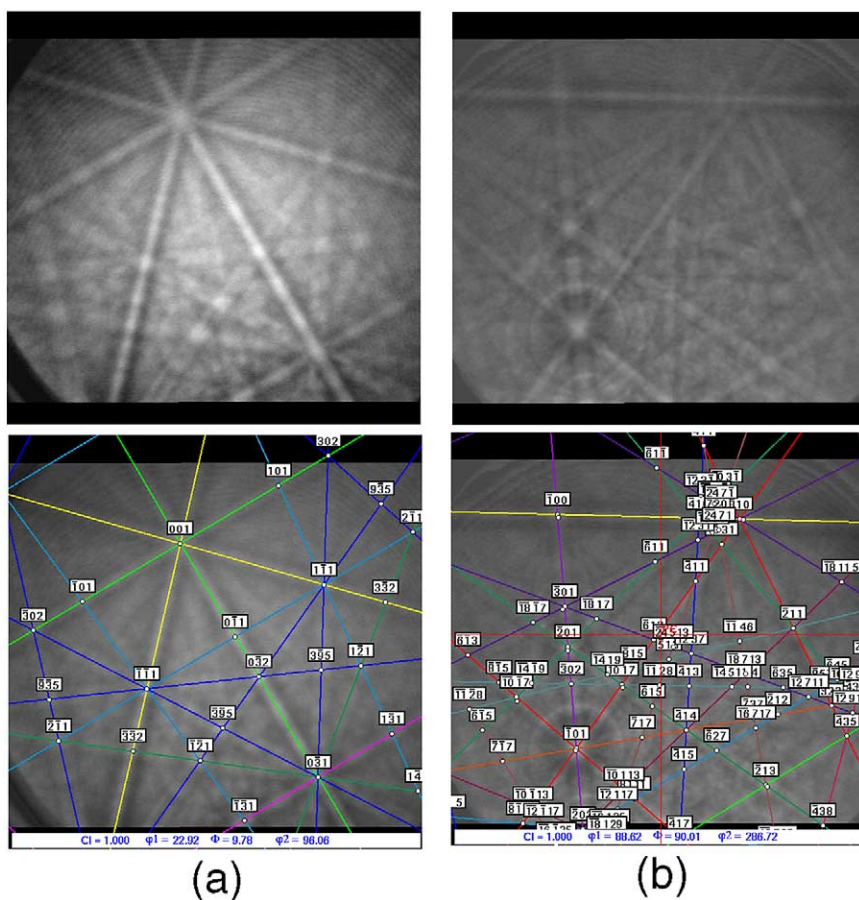


Fig. 1. Kikuchi patterns and indexation of YBCO (a) and Y-211 (b).

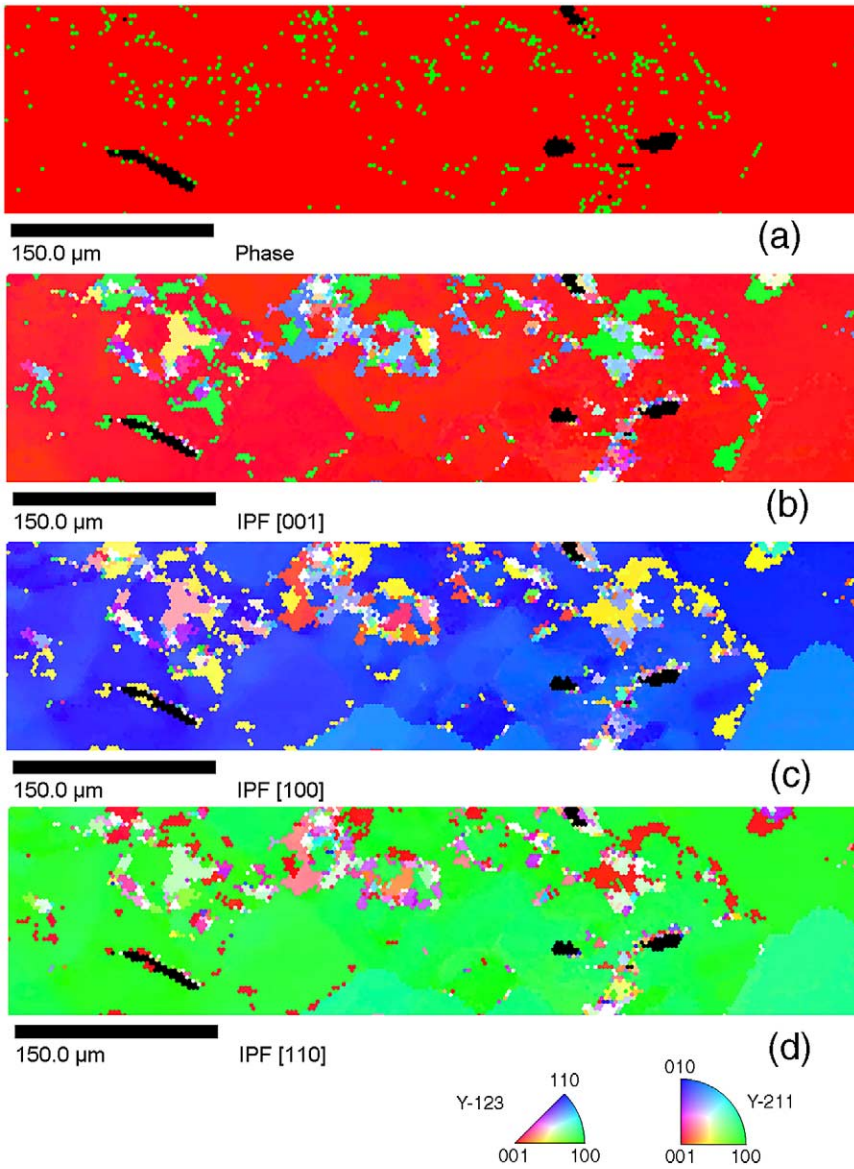


Fig. 2. OIM mapping. (a)–phase map, (b)–(d) IPF maps in $[0\ 0\ 1]$, $[1\ 0\ 0]$ and $[1\ 1\ 0]$ directions, respectively. The crystallographic orientations are given in the color-coded stereographic triangles for YBCO and Y-211.

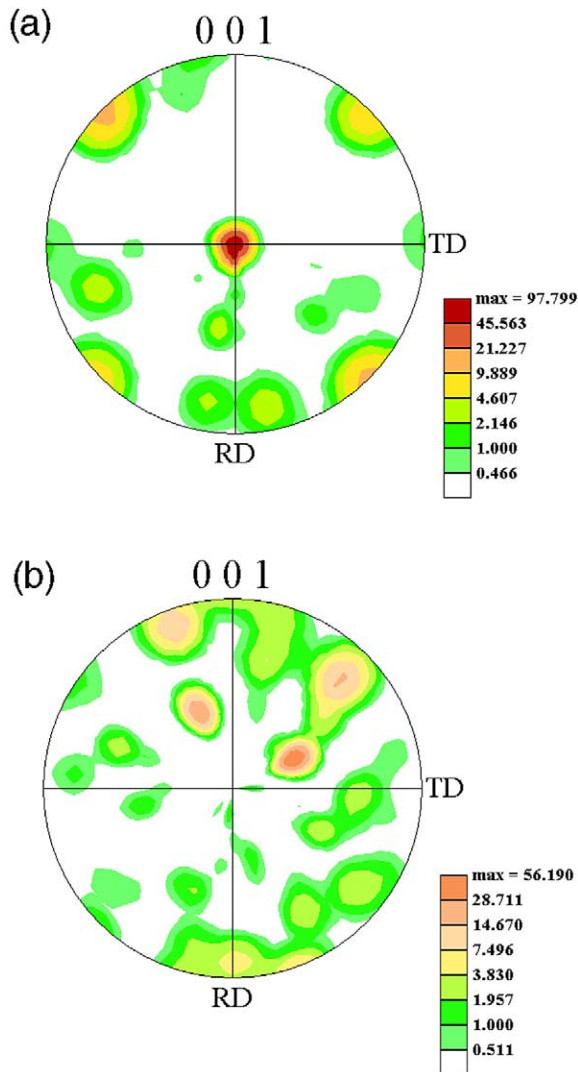


Fig. 3. Pole figures in $[0\ 0\ 1]$ direction for the YBCO phase (a) and the Y-211 phase (b).

the color-coded stereographic triangles for both phases. The well-developed c -axis $(0\ 0\ 1)$ texture of this sample is clearly demonstrated here, whereas the Y-211 phase does not exhibit any dominating direction. From the phase map, one can see that the Y-211 particles are often found close to cracks and voids in the bulk sample. Furthermore, the IPF maps reveal the subgrain structure of the sample. The subgrains are separated from the main grain by low-angle grain boundaries with angles up to 5° . A comparison of the phase map (a) and the IPF maps reveals further that the misoriented YBCO grains are located around the Y-211 particles, which indeed forms a severe obstacle for the homogeneous YBCO growth.

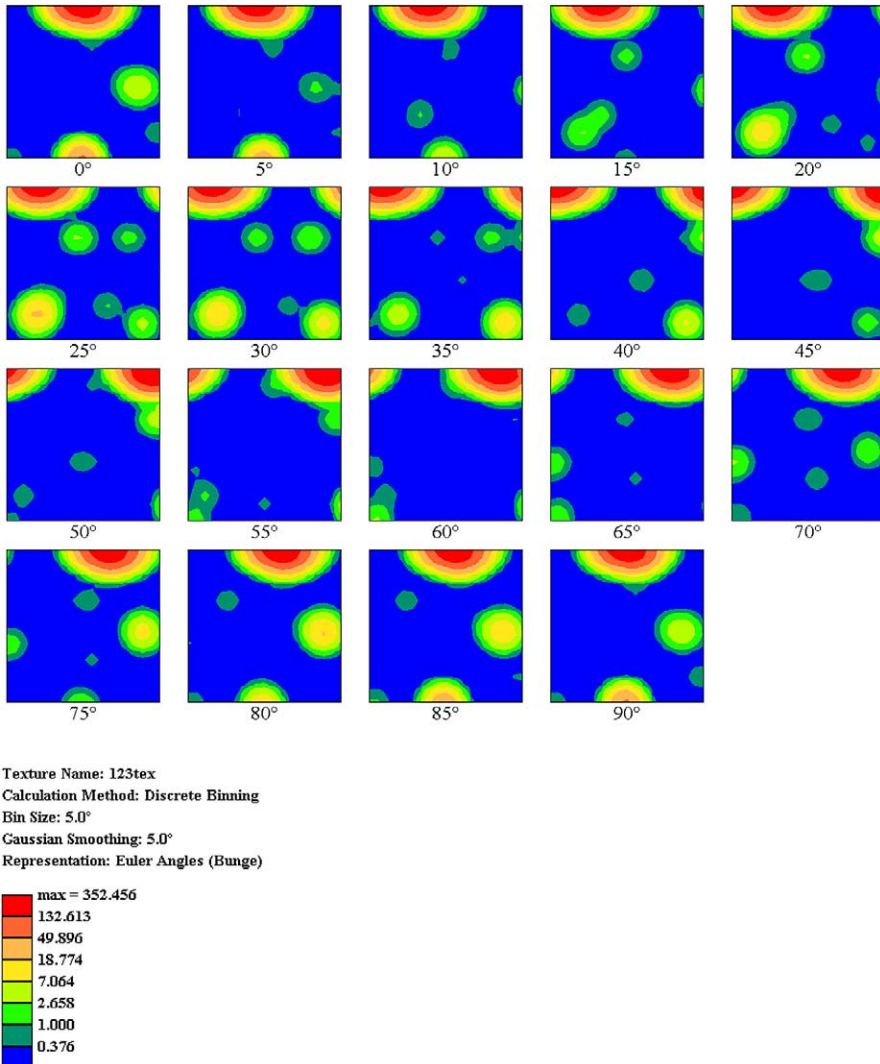


Fig. 4. ODF function for the YBCO phase.

Fig. 3 shows the corresponding pole figures in $[0\ 0\ 1]$ direction (= normal direction, ND) for both YBCO and Y-211, respectively. RD refers to the so-called reference direction along the sample tilt, and TD to the transverse direction. From these figures, it is again clearly visible that there is no dominant texture of the Y-211, whereas YBCO exhibits a clear $(0\ 0\ 1)$ or c -axis texture. Finally in Figs. 4 and 5, we present the calculated ODF functions for YBCO and the Y-211 phase, illustrating the strong texture of the melt-textured YBCO sample in $(0\ 0\ 1)$ direction. In contrast, the Y-211 phase does not exhibit any preferred grain orientation. We also see from the ODFs that the Y-211 particles are not oriented in $(1\ 0\ 0)$ or $(0\ 0\ 1)$ directions

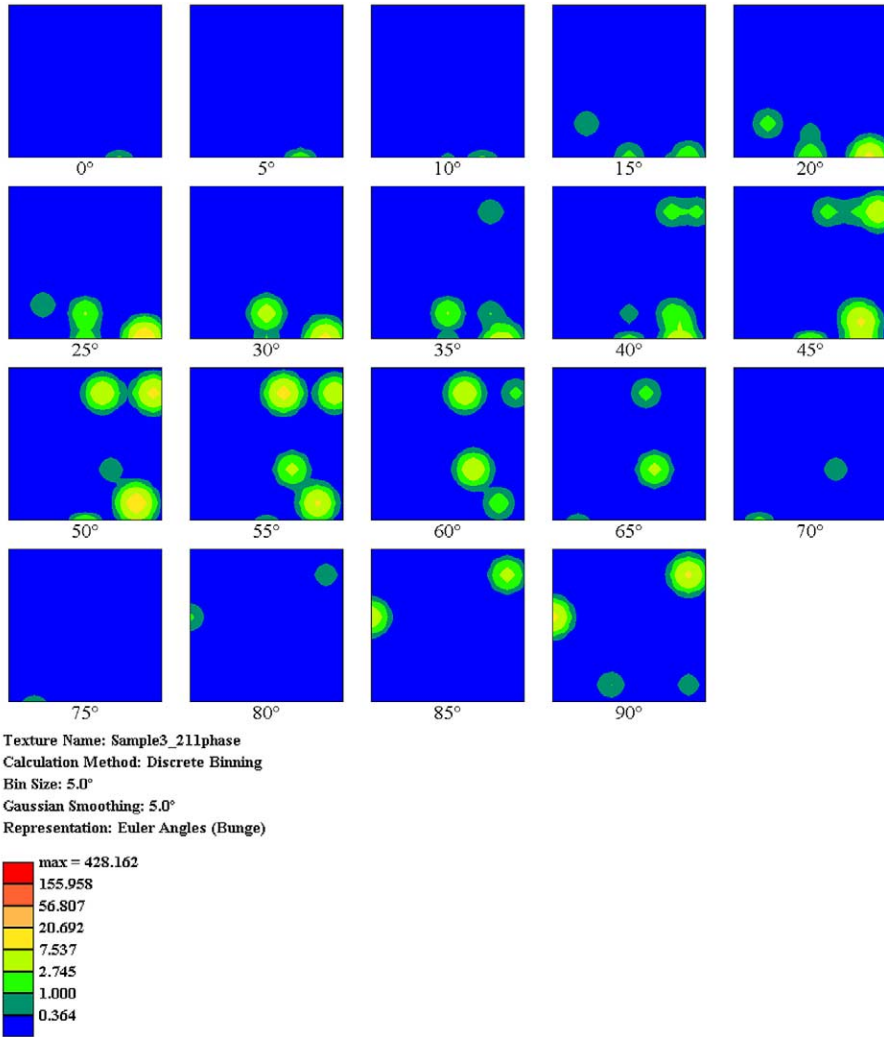


Fig. 5. ODF function for the Y-211 phase.

at all; the crystallites do evidently not fit together due to the different unit cell parameters, so intermediate orientations are preferred. From the two-phase mapping, we learn that between the Y-211 grains, the YBCO phase is not growing in (0 0 1) orientation, but shows also different orientations and correspondingly, small grains in order to accommodate the internal stresses due to the unit cell mismatch [10].

The interaction between the Y-211 and YBCO clearly reveals that it will be an essential task to further reduce the size of the Y-211 particles—especially to avoid the growth of large Y-211 particles completely. This will not only be beneficiary for the enhanced flux pinning properties, but also enable a more homogeneous growth of the YBCO phase.

4. Conclusions

OIM imaging was successfully applied to bulk, melt-textured YBCO samples. A two-phase analysis allows to study the interactions between YBCO and the Y-211 particles embedded in the YBCO matrix. We found that the presence of especially large Y-211 particles severely disturbs the homogeneous growth of the YBCO phase, thus a further reduction of the Y-211 particle size will be essential for the further development of melt-textured YBCO bulks.

Acknowledgements

AVK and MRK would like to thank the Japanese Science and Technology Agency (STA) for providing the fellowship for the stay at SRL/ISTEC. This work was performed as part of DFG project no. MU959/6.

References

- [1] M. Murakami, in: M. Murakami (Ed.), *Melt Processed High Temperature Superconductors*, World Scientific, Singapore, 1993.
- [2] P. Diko, *Supercond Sci Technol* 13 (2000) 1202.
- [3] K. Ogasawara, N. Sakai, M. Murakami, *Supercond Sci Technol* 13 (2000) 688.
- [4] D.J. Dingley, V. Randle, *J Mater Sci* 27 (1992) 4585.
- [5] R.A. Schwarzer, *Mat Sci Forum* 287-288 (1998) 23.
- [6] T. Fujimoto, M. Mitsuru, N. Masahashi, T. Kaneko, *IOP Conf. Ser.*, 167, Vol. 1, 2000, p. 79.
- [7] M. Murakami, N. Sakai, T. Higuchi, S.I. Yoo, *Supercond Sci Technol* 9 (1996) 1015.
- [8] A. Koblischka-Veneva, M.R. Koblischka, P. Simon, F. Mücklich, M. Murakami, *Supercond Sci Technol* 15 (2002) 796.
- [9] Orientation Imaging Microscopy software version V2.6, user manual, TSL, Draper, UT.
- [10] F. Sandiumenge, S. Pinol, X. Obradors, E. Snoeck, C. Roucau, *Phys Rev B* 50 (1994) 7032.